SENSITIVITY ANALYSIS OF ELECTROCHEMICAL IMPEDANCE UNDER BUBBLE-INDUCED AND FORCED CONVECTIONS

I. N. Bastos, W. L. Cardoso, J. F. V. Vasconcellos
Instituto Politécnico IPRJ, Universidade do Estado do Rio de Janeiro, UERJ, Caixa Postal 97282, 28601-970 Nova Friburgo RJ, Brasil. inbastos@iprj.uerj.br

F. Huet, R.P. Nogueira, C. Gabrielli
UPR15 du CNRS, "Laboratoire Interfaces et Systèmes Electrochimiques", Université Pierre et Marie Curie, C.P. 133,
4 Place Jussieu, 75252 Paris, Cedex 05, France. nogueira@ccr.jussieu.fr

Abstract. The aim of this paper is to analyze the sensitivity of parameters used in modeling the electrochemical impedance under bubble-induced and forced convections. Electrochemical impedance measurements have not been traditionally used in the presence of strong bubble evolution due to drift and noise occurrences. However, some works not only experimentally measured this system but also modeled it. The effects of current density and electrode speed modify the hydrodynamics and consequently the electrochemical impedance results. The present work analyzed the sensitivity of the electrochemical nature of parameters in the frequency domain.

**Keywords.** Sensitivity Analysis, EIS; Bubble Evolution; Forced Convection; Modeling

1. Introduction

The effects of the H_2 bubble evolution on mass and heat transfer in electrochemical cells have been studied in several experimental and theoretical works (Elsner and Marchiano, 1982; Shah and Jorne, 1989; Sutija and Tobias, 1994; Boissonneau and Byrne, 2000). However, electrochemical impedance spectroscopy –EIS measurements have not been extensively used because the presence of bubbles was usually considered as a source of drift and/or noise (Ekdune et all, 1991; Bai et all, 1987). For that reason, many of the works dealing with hydrogenic evolution reaction were limited to low current densities for which very few bubbles were evolved or a forced convection (rotating disc electrode) was employed to hydrodynamically avoid the presence of bubbles on the electrode surface. The influence of bubble evolution on electrochemical impedance diagrams was investigated by Gabrielli et all. (2002) in a large range of cathodic current densities on stationary Pt electrode in alkaline solutions with and without addition of a ferricyanide redox couple. Additionally to that, the interface was simulated by means of a simplified model in which ferricyanide reduction reaction takes place at Pt active sites not blocked by adsorbed hydrogen or bubbles. In the present work this model was studied by sensitivity analysis to provide quantitative answers about the dependencies of electrochemical and convection parameters on global impedance diagrams. This procedure is always advisable in order to understand complex models where some parameters are of difficult experimental acquisition. Therefore, its quantitative influence on model behavior has to be known for the frequency swept range. Despite the utility in evaluating models, this analysis is rarely used in the electrochemical field and few works are available in its literature.

2. Impedance Modeling

The aim of this paper is to investigate the combined influence of H_2 bubble evolution and forced convection on the impedance of Pt in NaOH and NaOH + $K_3[Fe(CN)_6]$ solutions. The interface was modeled by considering that ferricyanide reduction occurred on Pt active sites not blocked by adsorbed hydrogen or bubbles It is interesting to note that the ferricyanide reduction could not occur indistinctly at any point of the metallic surface, because of the electrode screening due to bubbles and also because of the blocking effect of adsorbed hydrogen. Hence, in a first attempt to model this complex system, the interface was modeled by taking into account the parallel and simultaneous reductions of both hydrogen and ferric ion species. The latter reduction was considered to take place on Pt active sites that were not blocked by the presence of adsorbed hydrogen or direct bubble screening.

Hydrogen production on metallic electrodes is often assumed to follow the Volmer-Heyrovsky model:

$$H_2O + e^- \xrightarrow{k_1} H_{ads} + OH^- \tag{1}$$

$$H_2O + H_{ads} + e^- \xrightarrow{k_2} H_2 + OH^- \tag{2}$$
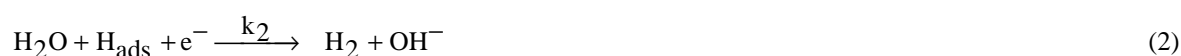
in alkaline media (Vetter, 1967), while ferricyanide, denoted Fe^{3+} for the sake of brevity, is reduced on the free surface according to the reaction:

$$Fe^{3+} + e^- \xrightarrow{\ k_3\ } Fe^{2+} \tag{3}$$

In the cathodic potential domain, only the forward reactions have been considered. Then, changes in the surface coverage, θ, by adsorbed hydrogen H_{ads} are governed by:

$$\beta \frac{d\theta}{dt} = k_1(1-\theta) - k_2\theta \tag{4}$$

where β is the maximum site number per unit surface. If the kinetic rate constants k_i are assumed to follow the Tafel law: $k_i = k_{io}\, e^{-b_i E}$ (i=1,2,3), the faradaic current is:

$$I_F = -F\left(k_1(1-\theta) + k_2\theta + k_3 c(0)(1-\theta)\right) \tag{5}$$

where c(x) is the concentration of Fe^{3+} in the solution, which obeys the Fick equation:

$$\frac{\partial c}{\partial t} = D\frac{\partial^2 c}{\partial x^2} \tag{6}$$

with the boundary conditions:

$$c(x = \delta\ \delta_N) = c^\infty \text{ and } D\frac{\partial c}{\partial x} = k_3 c(0)(1-\theta) \text{ at } x = 0 \tag{7}$$

where δ_N is the thickness of the Nernst diffusion layer. In steady-state conditions the surface coverage is:

$$\theta = \frac{k_1}{k_1 + k_2} \tag{8}$$

For small perturbations of the potential, ΔE, the interface response, $\Delta\theta$, is such that:

$$\Delta\theta = \frac{G\Delta E}{j\omega\beta + k_1 + k_2} \text{ with: } G = (b_2 - b_1)\frac{k_1 k_2}{k_1 + k_2} \tag{9}$$

while the concentration change, Δc, is given by Eq. (6) in the frequency domain:

$$j\omega\Delta c = D\frac{\partial^2 \Delta c}{\partial x^2} \tag{10}$$

with the boundary conditions:

$$\delta c(x = \delta_N) = 0 \tag{11a}$$

and

$$D\frac{\partial \Delta c}{\partial x}\bigg|_{x=0} = -b_3 k_3 c(0)(1-\theta)\Delta E + k_3(1-\theta)\Delta c(0) - k_3 c(0)\Delta\theta \tag{11b}$$

Hence, the faradaic current perturbation is:

$$\Delta I_F = R_t^{-1}\Delta E + F\left(k_1 - k_2 + k_3 c(0)\right)\Delta\theta - Fk_3(1-\theta)\Delta c(0) \tag{12}$$

where:

$$R_t^{-1} = F\left(b_1 k_1 (1-\theta) + b_2 k_2 \theta + b_3 k_3 (1-\theta)c(0)\right) \tag{13}$$

Finally, the faradaic impedance can be written, with $b = \sqrt{\dfrac{j\omega}{D}}$:

$$Z_F^{-1} = R_t^{-1} - F\,\frac{b_3 k_3^2 (1-\theta)^2 c(0)}{bD\coth(b\delta_N)+k_3(1-\theta)} +$$

$$F\left(k_1 - k_2 + k_3 c(0) - \frac{k_3^2(1-\theta)^2 c(0)}{bD\coth(b\delta_N)+k_3(1-\theta)}\right)\frac{G}{j\omega\beta + k_1 + k_2} \tag{14}$$

and the total impedance, Z, of the interface was obtained by taking into account the electrolyte resistance, R_e, and the double layer capacity, C_{dl}:

$$Z = R_e + \frac{Z_F}{1+j\omega C_{dl}Z_F} \tag{15}$$

Equation (15) is the general expression of the faradaic impedance when considering two parallel and simultaneous reactions of hydrogen and ferricyanide reduction. It can be checked that this model points out the existence of low-frequency loops associated to the relaxation of θ.

Table 1 – Parameters used for simulating the impedance diagrams in Fig. (1). The symbol sse stands for saturated sulfate electrode.

Parameters	$J_p - 7.5$ mA cm^{-2}	$J_p - 25.5$ mA cm^{-2}
E (Vsse)	- 0.185	- 0.240
k_{01} (mol cm^{-2} s^{-1})	5.5×10^{-11}	5.5×10^{-11}
k_{02} (mol cm^{-2} s^{-1})	8×10^{-8}	8×10^{-8}
k_{03} (mol cm^{-2} s^{-1})	0.2	0.2
b_1 (V^{-1})	33.5	33.5
b_2 (V^{-1})	3.5	3.5
b_3 (V^{-1})	2.5	2.5
C^∞ (mol cm^{-3})	1×10^{-4}	1×10^{-4}
β (mol cm^{-2})	6×10^{-9}	6×10^{-9}
θ (calculated from Eq. 8)	0.162	0.479
δ_N (cm)	200×10^{-4}	200×10^{-4}
D (cm^2 s^{-1})	100×10^{-6}	200×10^{-6}
C(0) (mol cm^{-3})	1×10^{-6}	0.5×10^{-6}
C_{dl} (µF)	30	80
R_e (Ohm.cm^2)	0.92	0.92

3. Comparison with Experimental Results

The existence of low-frequency loops occur, except when $b_1 = b_2$ (G = 0) or when $k_1 \to \infty$ ($\theta = 1$) or $k_2 \to \infty$ ($\theta = 0$). In the literature, these loops have been detected only in the absence of bubble evolution (low current-density (Ekdunge et all, 1991), or electrode rotation speed higher than 3600 rpm (Assunção et all. 1997). In the presence of bubbles, they have been obtained in this work in particular experimental conditions, depending on electrolyte stirring due to bubble evolution and electrode rotation. Simulation of Eq. (15) with the kinetic parameters given in Tab. 1 gives impedance diagrams with low-frequency loops show in Fig. 1. It should be noticed that these curves have been simulated by introducing arbitrary values of the ferricyanide concentration c(0) at the interface, because this quantity strongly depends on bubble evolution, giving values different from that derived from the diffusion boundary condition (Eq. (7). It is also expected that the diffusion coefficient D would be locally increased by electrolyte stirring due to bubble evolution, which enhanced mass transport. Hence, the parameters obtained from simulations must be considered as being averaged apparent values of diffusion coefficient, D, and diffusion layer thickness, δ_N, that simulate the effect of bubble evolution on ferricyanide mass transport. In this sense, the D values in Tab. (1), approximately 10 to 20 times higher than the usual value in bubble-free electrolyte, were considered, in this preliminary approach, to be reasonable values concerning forced and bubble-induced convections.

A direct comparison of experimental and simulated impedances is presented in Fig. (1) with, as an example, the Nyquist diagram corresponding to the experimental curve and the corresponding simulated curve confirming the good agreement in the whole frequency range. The model proposed above was able to simulate experimental results when considering that the ferricyanide reduction takes place at actives sites not blocked by adsorbed hydrogen. It seems then that the ferricyanide species act as a tracer to indirectly reveal the relaxation of H_{ads} that is hardly found in standard impedance measurements.

Due to uncertainties of actual values of some parameters deemed necessary to study how they affect the impedance in the experimental frequency range in order to have reliable values; this procedure, provided by sensitivity analysis, adds insight into the behavior of kinetic model.
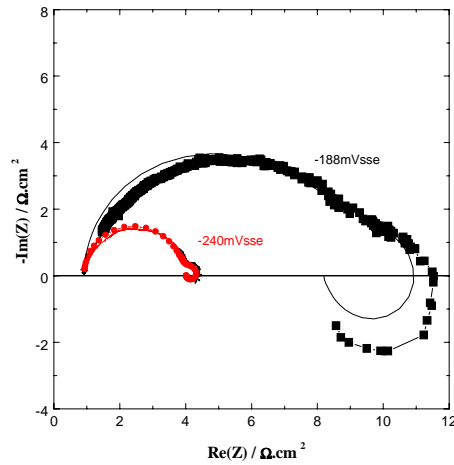

Figure 1. Experimental and modeled impedance. E = -185 mVsse and –240 mVsse.

4. Sensitivity Analysis

An important requirement in parameter estimation is that the sensitivity coefficients should not be of small magnitude, and when two or more parameters are estimated simultaneously, their sensitivity coefficients must be linearly independent over the experimental time or frequency domain (Beck *et alii*, 1985; Bieniasz and Speiser, 1998). Similar shapes (time or frequency dependence) of sensitivity coefficients for two or more different parameters indicate that their effects on the model response are similar, being, therefore, impossible to tell them apart. Larger sensitivity coefficients are related to better chances of obtaining good estimates. In the present work, we analyze the scaled sensitivity coefficients, which are defined as

$$X_s(t) = \beta_s \frac{\partial C_b(t)}{\partial \beta_s} \quad , \text{s= } 1, 2, ..., Np \tag{16}$$

where β_s are the parameters used in the present sensitivity analyses and may be one of these thirteen parameters: $\{E, b_1, b_2, b_3, K_{01}, K_{02}, K_{03}, \beta, C(0), C_{dl}, D, \lambda_N, R_e\}$. As it can be observed in Eq. (17), the scaled sensitivity coefficients have all the same units of Ohm.cm^2 for modulus and degree for phase angle, and a direct comparison is therefore possible. The sensitivity coefficients were calculated using a numerical approximation

$$\frac{\partial C_b(t)}{\partial \beta_s} = \frac{C_b\left(\beta_1, \beta_2, \cdots, \beta_s + \Delta\beta_s, \cdots, \beta_{Np}\right) - C_b\left(\beta_1, \beta_2, \cdots, \beta_s - \Delta\beta_s, \cdots, \beta_{Np}\right)}{2\Delta\beta_s}, \quad s = 1, 2, ..., Np \qquad (17)$$

In order to calculate the normalized sensitivity coefficients, approximate values of β_s are needed, as depicted in Tab. (1). We have calculated the sensitivity coefficients considering measured parameters that agree with experimental results in two electrochemical potentials, E = -185 and –240 mVsse (see Fig. (1)).
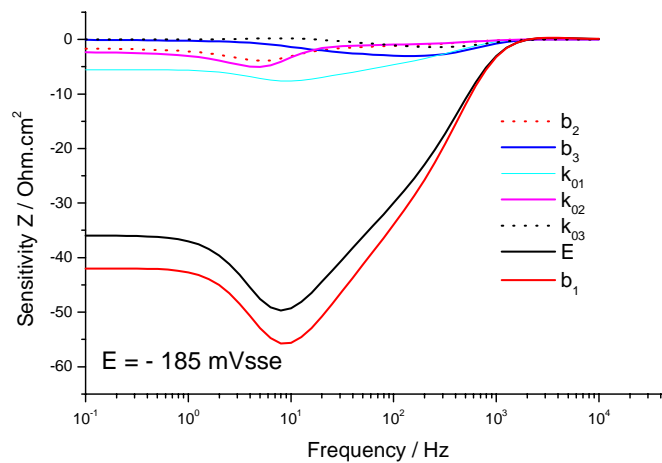

Figure 2. Sensitivity analyses for diagram. E = –185mVsse.

Figure (2) displays the scaled sensitivity coefficients at E= -185 mVsse. Our attention is consequently directed to E and b_1 due to their strong effect on the result. The parallelism observed in the curve possibly indicates some linear dependence between both. The analysis presented in Fig. 2 reveals the strong effect of potential and b_1 on impedance modulus for the potential of –185mVsse. Besides the fact that these two parameters have the most relevant sensitivity in the whole frequency range, around 10Hz their effect reaches the maximum. b_1 is the parameter related to reaction of adsorbed hydrogen production from water and plays a fundamental role in the alkaline medium without mass control. The coupling between E and b1 shows an apparent dependence for all frequencies. However, by calculating the difference of sensitivity between them, it is possible to assure a linear independence at least in the range from 5 Hz to 1KHz, as depicted in Fig. (3). This simple calculus consists of subtracting the sensitivity of E from b_1, for each frequency. Therefore, by employing this result and the model (Eq.(15)) we can determine the frequency range where the biggest sensitivity occurs and the experimental test should be carried out, if possible. These analyses can be extended for each parameter in respect to the others. K_{01} is the third most important parameter. Electrochemically this result is expected, since the majority of cathodic current in this case passes through hydrogen evolution, in spite of the parallel and simultaneous redox Fe^{3+}/Fe^{2+} reaction. This redox reaction has small impact on the impedance modulus, as shown by its small sensitivity of b_3 and K_{03}. This is also in good agreement with the electrochemical model, since the redox reaction is supposed not to take place at reactive sites blocked by adsorbed hydrogen. The negative values of sensitivity indicate a trend in decreasing the modulus of impedance. The vice-versa is also true.
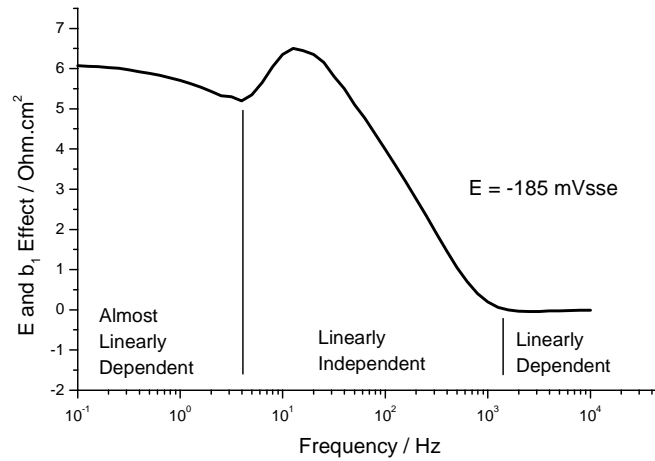
Figure 3. Dependence between E and b_1. E = -185 mVsse.

The influence of small potential steps in modifying the diagram is shown in Fig. (4). In this case the small difference of only 3mV produces a different Nyquist diagram. Usually the present sensitivity affects negatively the modulus, thus the increasing absolute value in potential has an effect of decreasing the modulus. Indeed, this is observed in simulation showed in Fig. (4). In experimental impedance testing is usual to employ a perturbation signal with amplitude around 10mV. For systems with high sensitivity in respect to potential, there should be expected some difference mainly in low frequency domain. The difference between experimental and simulated Nyquist diagrams in low frequency presented in Fig. (1) is probably due to this influence.
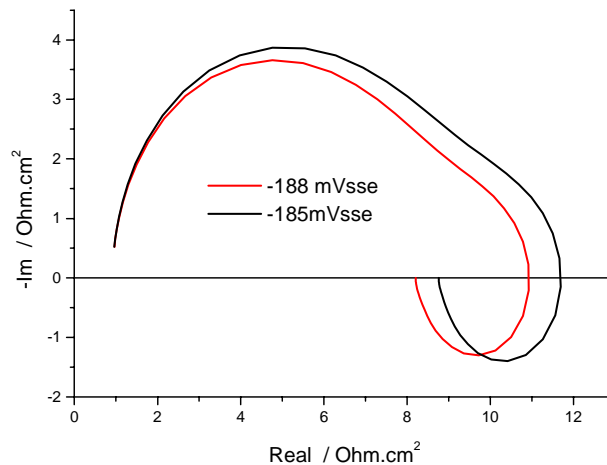

Figure 4. Strong effect of potential on Nyquist diagram. E = -185 and –188 mVsse.

In Fig. (5) the sensitivity coefficients for $\{\beta, C(0), C_{dl}, D, \lambda_N\}$ parameters is shown. It is observed that they have minor magnitude. However, this behavior does not imply that they are unimportant. A useful result can occur if some of them present difficulties to be experimentally obtained. In the present case we can mention D, C(0) and δ_n, where a direct relationship with the electrochemical process is coupled with cumbersome mass transport phenomena. Therefore, for these parameters, approximated values do not jeopardize the simulation quality, and additional efforts to obtain accurate values are not advisable. This result corroborates the approximated D values assumed before.
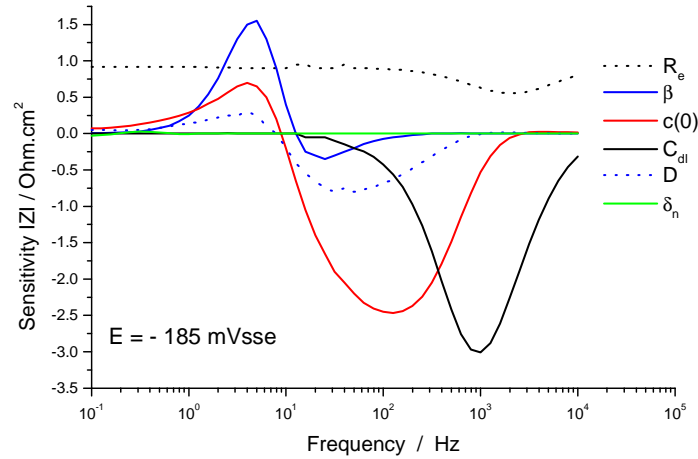
Figure 5. Sensitivity analysis for modulus diagram. E = –185mVsse.

Some parameters have positive effects on the modulus, such as Re and β. C_{dl} reaches the highest effect around 1 KHz as should be expected for double layer capacity, which affects the impedance behavior in high frequency.
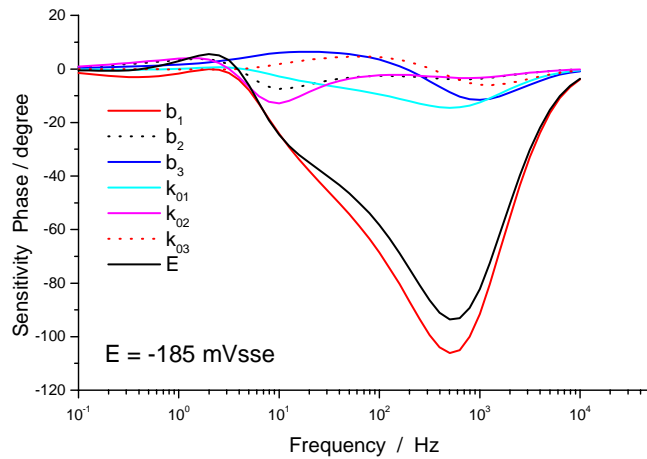

Figure 6. Sensitivity analysis for phase angle. E = –185mVsse.

An impedance diagram is usually presented in Bode (modulus and phase angle) or Nyquist (real and imaginary components). Although they have the same amount of information, some authors strongly recommend the Bode plots (Mansfeld, 1988) because all points are displayed equally. Therefore, the analysis has to take into account the angle sensitivity. Fig. (6) shows how the parameters affect the angle. A similar influence of E and b_1 is found when considering the parameters $\{E, b_1, b_2, b_3, K_{01}, K_{02}, K_{03}\}$. The $\{\beta, C(0), C_{dl}, D, \lambda_N\}$ parameters affect in an almost totally linear independent manner the phase angle, despite the fact of their minor magnitude as a whole. Re and C_{dl} are far more responsible for the closing of the Nyquist plot near 10KHz, where the diagram is completely reduced to Re.

For the potential of –240mVsse the strong effect of b_1 and E is still quite relevant. However, b_2 and k_{02} have a strong influence than the one at –185mVsse owing to the higher adsorbed hydrogen coverage. Indeed, reaction (2) acts by liberating blocked sites that can further react by reactions (1) or (3), which subsequently affect the overall impedance modulus. Besides, K_{02} and b_2 parameters are linearly dependent for all frequencies.
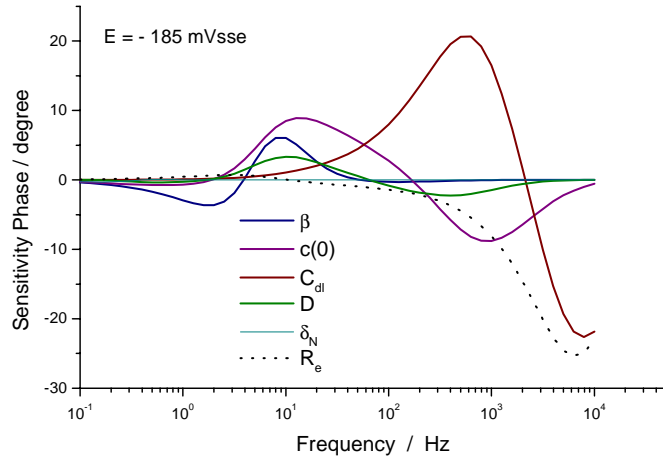
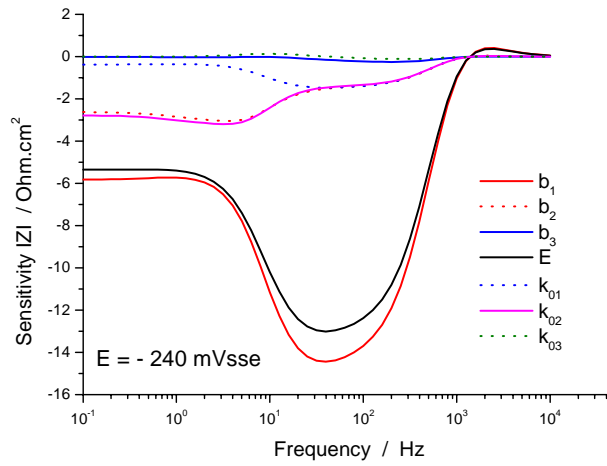Figure 7. Sensitivity analysis for phase plot. E = –185mVsse.

Figure 8. Sensitivity analysis for modulus diagram. E = –240mVsse.
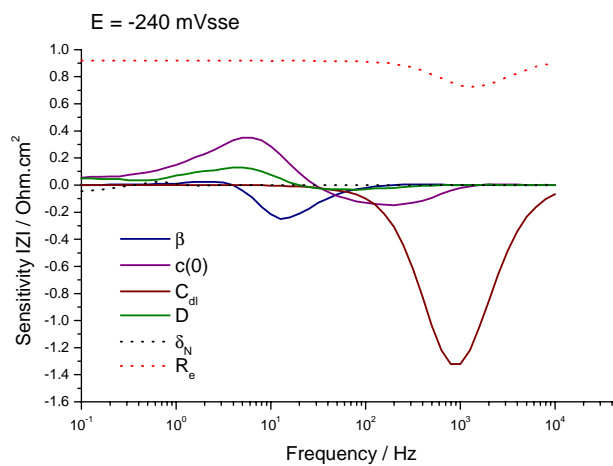

Figure 9. Sensitivity analysis. E = –240mVsse.

The parameters $\{b_1, b_2, b_3, k_{01}, k_{02}, k_{03}, \delta_n, \beta\}$ are constant in both potentials. Otherwise, their sensitivities are different for each potential and frequency range. As an example, the effect of C(0) is relevant from 1Hz to 1KHz at –185 mVsse, as depicted in fig. 5. On the other hand, for –240mVsse its sensitivity vanishes or has a small positive

signal in the same region, as shown in fig.9. So, the experiment and simulation with interest in this parameter is more sensitivity to be carried out at –185mVsse than 240mVsse.

The inverse problem, not performed here, consists in finding more reliable values for a given experimental impedance diagram and mathematical formulation. This procedure is always advisable for multiparameter models, typical of complex physical systems.

5. Conclusions

The use of sensitivity analysis methods in the modeling of electrochemical impedance provides additional information about the dependence of parameters during the frequency sweep. This approach proved useful especially in this electrochemical system, not extensively studied by impedance, due to the drift and noise caused by the bubbles. The analyses showed the strong effect of potential and Tafel coefficients that almost control the overall kinetic process even in the presence of a rotating electrode.

6. References

Assunção, N. A.; Giz, M. J.; Tremiliosi-Filho, G.; Gonzáles, E. R., 2000, J. Electrochem. Soc., N.144, pp.767.

Bai, L.; Harrington, A. and Conway, B. E., 1987, Electrochim. Acta, 32, pp.1713.

Beck, J. V., Blackwell, B. and St. Clair Jr., C. R., 1985, Inverse Heat Conduction, Wiley, New York.

Bieniasz, L. K.; Speiser, B., 1998, Journal of Electroanalytical Chemistry, N.441, pp.271-285.

Boissonneau, P. and Byrne, P., 2000, J. Appl. Electrochem., 30, pp.767.

Eigeldinger, J. and Vogt, H., 2000, Electrochim. Acta, N.45, pp.4449.

Ekdunge, P.; Jüttner, K.; Kreysa, G.; T. Kessler, T.; Ebert, M. and Lorenz, W. J., 1991, J. Electrochem. Soc., N.138, pp.2660.

Elsner, C. and Marchiano, L., 1982, J. Appl. Electrochem., N.12, pp.735.

Gabrielli, C.; Huet, F. and Nogueira, R. P., 2002, Electrochim. Acta, N.47, pp.2043-2048.

Mansfeld, F., 1988, Corrosion, V.44, N. 8, 558-559.

Shah, A. and Jorne, J., 1989, J. Electrochem. Soc., N.136, pp.153.

Sutija, D. P. and Tobias, C. W., 1994, J. Electrochem. Soc., V.141, pp.2599.

Vetter, K. J., 1967, Electrochemical Kinetics, Academic Press, New York.